APL Materials

Enhanced photovoltaic performance of perovskite solar cells by Co-doped spinel nickel cobaltite hole transporting layer

Cite as: APL Mater. 7, 021101 (2019); https://doi.org/10.1063/1.5079954
Submitted: 05 November 2018 . Accepted: 08 January 2019 . Published Online: 06 February 2019

Apostolos Ioakeimidis, Ioannis T. Papadas, Dimitris Tsikritzis, Gerasimos S. Armatas, Stella Kennou, and Stelios A. Choulis

Enhanced photovoltaic performance of perovskite solar cells by Co-doped spinel nickel cobaltite hole transporting layer

Cite as: APL Mater. 7, 021101 (2019); doi: 10.1063/1.5079954
Submitted: 5 November 2018 • Accepted: 8 January 2019 •
Published Online: 6 February 2019

Apostolos Ioakeimidis,[1] Ioannis T. Papadas,[1] Dimitris Tsikritzis,[1] Gerasimos S. Armatas,[2] Stella Kennou,[3] and Stelios A. Choulis[1,a)]

AFFILIATIONS

[1]Molecular Electronics and Photonics Research Unit, Department of Mechanical Engineering and Materials Science and Engineering, Cyprus University of Technology, Limassol 3603, Cyprus
[2]Department of Materials Science and Technology, University of Crete, Heraklion 71003, Greece
[3]Department of Chemical Engineering, University of Patras, 26504 Patras, Greece

[a)]**Author to whom correspondence should be addressed:** stelios.choulis@cut.ac.cy

ABSTRACT

A solution combustion synthesized hole transport layer (HTL) of spinel nickel cobaltite ($NiCo_2O_4$) incorporating 3% Cu–2% Li was fabricated using the doctor-blading technique for planar inverted perovskite solar cells (PVSCs). PVSCs incorporating 3% Cu–2% Li-doped $NiCo_2O_4$ showed an increase in Jsc and Voc device performance parameters compared to unmodified $NiCo_2O_4$, leading to power conversion efficiency (PCE) of 16.5%. X-ray photoelectron spectroscopy measurements revealed the tendency of Cu cations to replace preferably the surface Ni atoms by changing the surface stoichiometry of $NiCo_2O_4$, inducing a cathodic polarization. Ultraviolet photoelectron spectroscopy measurements unveiled the increase in the ionization potential by 0.1 eV for a co-doped $NiCo_2O_4$ film compared to unmodified $NiCo_2O_4$-based HTL. We attribute the enhanced PCE of the inverted PVSCs presented to the improved hole extraction properties of 3% Cu–2% Li $NiCo_2O_4$ HTL.

Perovskite solar cells (PVSCs) have shown an incredible fast power conversion efficiency (PCE) improvement, going from 3.8% in 2009[1] to over 20% in 2018.[2–5] A lot of parameters have been investigated to increase the performance and reliability of the devices, such as the element composition[6–11] and preparation method of perovskite,[12–21] device configuration,[22–26] and materials and preparation conditions of hole/electron transporting layers.[27–33]

Regarding the investigation of functional hole transporting layers (HTLs), a wide variety of organic and inorganic materials have been implemented to improve hole extraction, with some of the latter's advantage being the wide optical band gap (thus high transparency in the visible range) and superior hole mobility, while they can be solution processed. Some promising inorganic HTLs are NiOx,[34] Cu:NiOx,[35–37] CuOx,[38–40] CuI,[41] CuSCN,[42] $CuGaO_2$,[43] and $CuCrO_2$.[44] Recently, we have reported combustion synthesis of monodispersed spinel $NiCo_2O_4$ nanoparticles of ~4 nm diameter forming a compact layer with an electrical conductivity of ~4 S/cm. The developed films were applied as an efficient and reliable HTL for inverted structure perovskite solar cells (PVSCs) using a 230 nm thick perovskite layer.[45] In order to increase the PCE of the devices, a thicker perovskite layer is needed. The enhancement in light absorption leads to an increase in photogenerated carriers which accumulate at the perovskite/HTL interface (accumulation zone) and are subsequently collected by the contact.[46] Thus, HTLs with enhanced hole collection capability are required to increase the PCE. A common method to enhance HTL charge collection efficiency is incorporation of intentional defects through extrinsic doping. This process can induce a higher electrical conductivity as well as better energy level alignment

of HTL with the perovskite active layer.[47–51] For example, recently a co-doping strategy of NiOx with Cu/Li or Li/Mg elements has been successfully applied to enhance the PCE of PVSC.[52,53]

In this paper, we report the use of solution combustion synthesized $NiCo_2O_4$ co-doped with 3 mol. % Cu and 2 mol. % Li (3% Cu–2% Li) as efficient HTL to increase the performance of inverted PVSCs. Initially, a $NiCo_2O_4$ film doped with 5 mol. % Cu was incorporated as HTL in PVSC exhibiting an increased Voc. However, the Jsc of the corresponding PVSC has declined significantly compared to unmodified $NiCo_2O_4$-based PVSC due to lower electrical conductivity. We show that an increase in the electrical conductivity can be achieved by 3% Cu and 2% Li co-doping of the $NiCo_2O_4$-HTL, resulting in PVSCs with enhancement on both Voc and Jsc compared to $NiCo_2O_4$-HTL based PVSCs.

X-ray photoelectron spectroscopy(XPS) investigation on co-doped $NiCo_2O_4$-HTL showed a decrease in the Ni/Co atomic ratio compared to unmodified $NiCo_2O_4$-HTL, indicating the preferable surface substitution of nickel by copper cations, which induces a cathodic polarization as has been previously reported.[54] As a result, an increase in the ionization potential by 0.1 eV was observed for 3% Cu–2% Li $NiCo_2O_4$-HTLs compared to stoichiometric $NiCo_2O_4$-HTL using ultraviolet photoelectron spectroscopy (UPS). The increased performance of the reported PVSCs could be attributed to the cathodic polarization potential and thus better hole collection efficiency of the 3% Cu–2% Li $NiCo_2O_4$ layer.

The PVSCs under investigation were prepared on top of glass/Indium Tin Oxide (ITO)/$NiCo_2O_4$ for the different doping types processed as described in detail in the supplementary material. The perovskite solution was prepared 30 min prior to spin coating by mixing $Pb(CH_3CO_2)_2.3H_2O$:methylammonium iodide (1:3) at 40 wt. % in dimethylformamide (DMF) with the addition of 1.5% mole of MABr (methylammonium bromide). Briefly, an ~350 nm perovskite active layer was spin-coated on top of each substrate followed by 50 nm spin-coated $PC_{70}BM$ (serving as the electron selective contact) and 100 nm thermally deposited Al. More details of the materials and processing conditions can be found in the supplementary material.

Figure 1(b) demonstrates the current density-voltage (J–V) measurements under 1 sun simulated illumination for the PVSCs using $NiCo_2O_4$ with different doping types, and the extracted photovoltaic parameters are shown in Table I. Pristine $NiCo_2O_4$ HTL based PVSCs show a considerably lower Voc (0.88 V) but higher Jsc (18.25 mA/cm^2) compared to 5% Cu-doped $NiCo_2O_4$ HTL based PVSCs (Voc = 1.03 V, Jsc = 14.89 mA/cm^2), while FF is similar (72.3% and 73%), delivering a PCE of 11.61% and 11.02%, respectively. Importantly, PVSCs incorporating 3% Cu–2% Li $NiCo_2O_4$ HTL exhibit both higher Voc (1.05 V) and Jsc (21.05 mA/cm^2) as well as a slightly higher FF (74.8%) compared to previous devices, delivering a PCE of 16.54%.

In order to investigate the reduced photocurrent of 5% Cu-doped $NiCo_2O_4$, we first excluded any possible optical

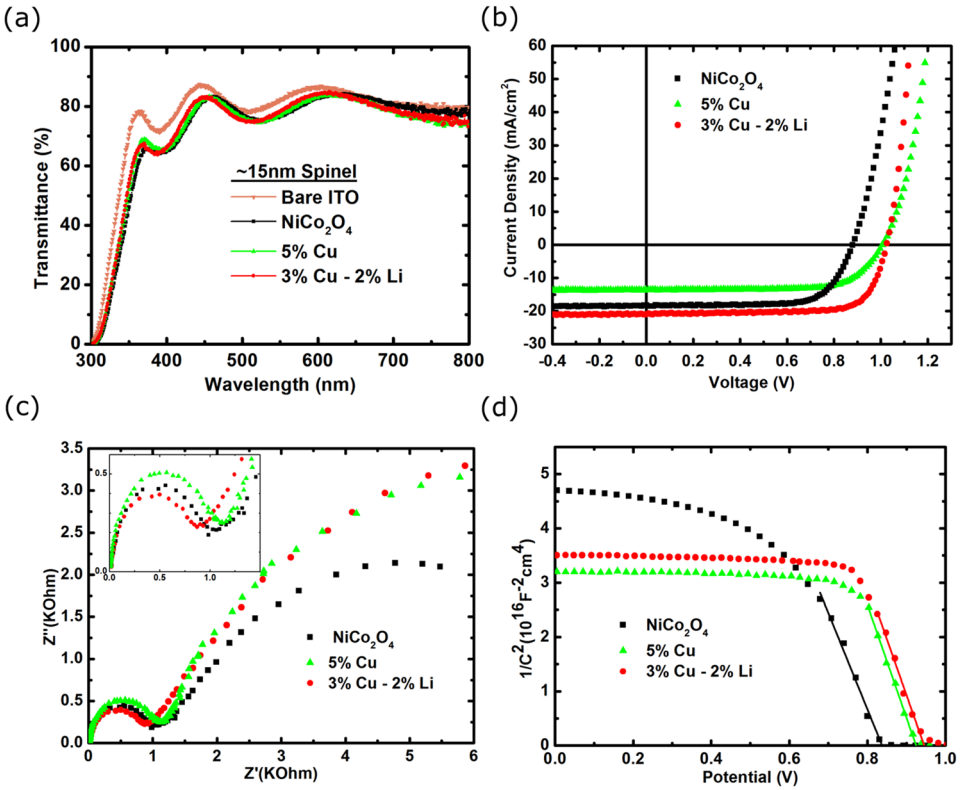

FIG. 1. (a) Transmittance measurements of bare glass/ITO and different types of doped 15 nm $NiCo_2O_4$ fabricated on glass/ITO substrates. (b) J-V curves and (c) Nyquist (inset: zoomed-in view at the high frequency region) and (d) Mott-Schottky plots of PVSC using 15 nm undoped, 5% Cu, and 3% Cu–2% Li doped $NiCo_2O_4$ HTL.

TABLE I. J-V extracted parameters of PVSC using 15 nm undoped, 5% Cu, and 3% Cu–2% Li $NiCo_2O_4$ as HTL.

HTL	Voc (V)	Jsc (mA/cm^2)	FF (%)	PCE (%)
$NiCo_2O_4$	0.88	18.25	72.3	11.61
5% Cu	1.03	14.89	73	11.02
3% Cu–2% Li	1.05	21.05	74.8	16.54

TABLE II. Room-temperature four-point probe extracted values of undoped $NiCo_2O_4$ and 5% Cu and 3% Cu–2% Li $NiCo_2O_4$ films.

$NiCo_2O_4$	Conductivity (S/cm)
Undoped	4.00
5% Cu	1.87
3% Cu–2% Li	4.85

losses induced by the doping. Figure 1(a) demonstrates the transmittance of an ~15 nm-thick $NiCo_2O_4$ layer on glass/ITO. It is obvious that the difference in transmittance is negligible for all films under study, where the extracted Tauc-plot (Fig. S1) for direct transitions $[(\alpha.E)^2 = A.(E - Eg)]$ shows similar optical bandgaps (Egs). Furthermore, the similar morphology in all types of $NiCo_2O_4$ films was confirmed excluding, also, differences in electrical losses related to film quality (e.g., shunting current). Figures S2 and S3 illustrate the AFM topography images of (a) 5% Cu and (b) 3% Cu–2% Li $NiCo_2O_4$ films fabricated on quartz and glass/ITO substrates, while Fig. S3(c) illustrates the topography of the ITO underlayer. In both cases, the films exhibit similar roughness between them (0.7–0.8 nm for quartz and 2.9–3.0 nm for glass/ITO substrates) comparable to the ones measured for the pristine $NiCo_2O_4$ films, affirming the similar quality of different types of $NiCo_2O_4$ films.[45]

Thus, electrical characterization of PVSC was performed using electroimpedance spectroscopy (EIS) measurements under illumination and zero bias on the previously described PVSC configurations. As it is observed in Fig. 1(c), all spectra show the characteristic two frequency response, where the first arc (higher frequencies) is ascribed to charge transport resistance (R_{tr}), while the second larger arc (lower frequencies) is ascribed to the charge carrier recombination resistance (R_{rec}).[55,56] PVSC incorporating 3% Cu–2% Li $NiCo_2O_4$-HTL exhibits higher R_{rec} compared to unmodified $NiCo_2O_4$-HTL based PVSCs, while showing lower R_{tr} [Fig. 1(c), inset)]compared to both unmodified and 5% Cu-doped $NiCo_2O_4$-HTL based PVSCs due to the higher electrical conductivity of the 3% Cu–2% Li $NiCo_2O_4$ layer, as it was also confirmed by the four point probe conductivity measurements summarized in Table II. Kim *et al.* also reported an increase in the electrical conductivity of spinel nickel cobaltite by introduction of Li.[57]

Additional Mott-Schottky [Fig. 1(d)] measurements were carried out on devices sweeping from higher to lower voltage under dark conditions. The crossing of the curves at $1/C^2 = 0$ is attributed to the flat band potential of the device.[58,59] 5% Cu and 3% Cu–2% Li $NiCo_2O_4$-HTL based PVSCs show a higher built-in potential compared to unmodified $NiCo_2O_4$-HTL based PVSCs, which is consistent with the increased Voc value achieved for the 5% Cu and 3% Cu–2% Li NiCo2O4-HTL based PVSCs.

Further investigation of the charge carrier recombination dynamics was conducted to elucidate the enhanced device performance of 3% Cu–2% Li doped $NiCo_2O_4$-HTL based PVSCs compared to undoped $NiCo_2O_4$-HTL based PVSCs. We first exclude any difference in the perovskite film morphology. AFM topography images (Fig. S4) of the perovskite surface revealed similar surface roughness (12.5 ± 0.4 nm) and grain sizes (~110-123 nm), as shown in the supplementary material (Fig. S5), indicating that PVSCs under study comprise similar morphology within the active layer. Moreover, Voc-light intensity measurements were performed to investigate the recombination mechanism within PVSCs under study. According to the simplified Shockley-Read-Hall recombination model, the slope between logarithmic light intensity and

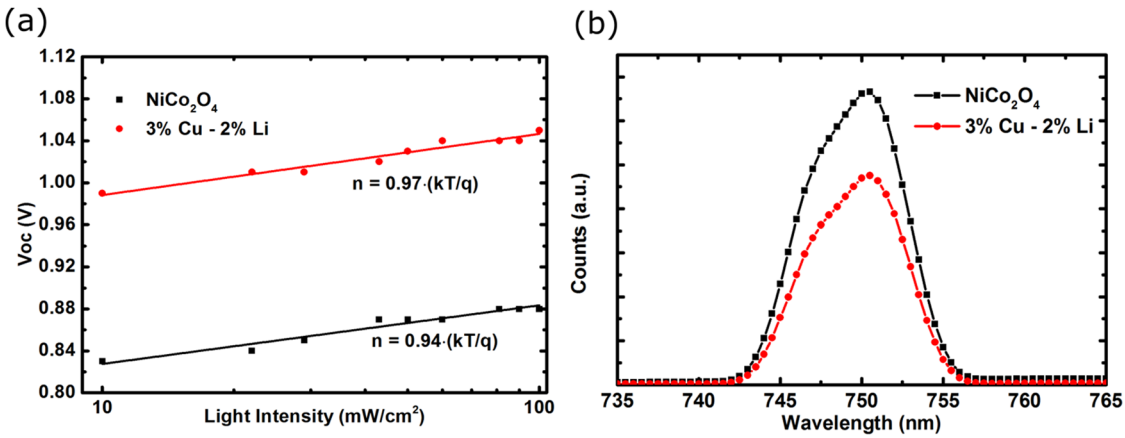

FIG. 2. (a) Voc–light intensity measurements of PVSC using 15 nm-sized undoped and 3% Cu–2% Li HTL. (b) Steady-state room temperature photoluminescence (PL) spectra of 350 nm thick perovskite films fabricated on 15 nm unmodified and 3% Cu–2% Li co-doped $NiCo_2O_4$ on a glass/ITO substrate.

TABLE III. Nickel to cobalt (Ni:Co) ratio obtained by the XPS analysis of undoped, 5% Cu, and 3% Cu–2% Li $NiCo_2O_4$ samples.

Ratio	$NiCo_2O_4$	5% Cu	3% Cu–2% Li
Ni:Co	0.55	0.43	0.45

Voc must be equal to 2kT/q for trap-assisted and kT/q for trap-free recombination.[60–64] As shown in Fig. 2(a), the Voc-light intensity curves scale equal to kT/q, implying that a trap-free recombination mechanism is dominant for all the PVSCs in this paper. Thus, steady state photoluminescence (PL) measurements [Fig. 2(b)] are adequate to evaluate the degree of charge recombination at each configuration. The PL intensity of undoped $NiCo_2O_4$-HTL is much higher compared to 3% Cu–2% Li $NiCo_2O_4$-HTL, implying that a much higher number of electron-hole pairs recombine for the case of the undoped HTL, justifying the lower PCE of the corresponding undoped NiCo2O4-HTL based PVSCs. The experimental results presented indicate that 3% Cu–2% Li $NiCo_2O_4$ HTL transfers and collects hole charges more efficiently than the undoped $NiCo_2O_4$ HTL.

A deeper material property and device physics investigation was performed to better understand the origin of the enhanced hole collection properties of 3% Cu–2% Li $NiCo_2O_4$. Structural characterization with X-ray diffraction (XRD) on the corresponding $NiCo_2O_4$ samples (Fig. S6) matched the cubic face-centered lattice structure of $NiCo_2O_4$ (PDF#20-0781), implying single-crystalline structure. X-ray photoelectron spectroscopy (XPS) measurements were also performed on doped and undoped $NiCo_2O_4$ HTLs. The Co 2p spectrum (Fig. S7) was best fitted by using two spin-orbit doublets for the tetrahedral Co^{+2} and octahedral Co^{+3} oxidation states and with two shake-up satellites located at the higher binding energy (BE) side of the main peaks. The peak located around 779.7 eV can be attributed to the octahedral Co^{+3} observed in Co_3O_4,[65] while the higher binging energy peak around 780.9 eV can be assigned to the tetrahedral Co^{+2} similar to CoO.[66] The spectrum of the Ni $2p_{3/2}$ region was fitted using three components (Fig. S8). The peak at 854.3 eV corresponds to Ni^{+2} ions, while that at 856.0 eV is attributed to Ni^{+3}.[65,67] The shake-up satellite at around 861.8 eV was fitted considering one broad line. For Cu doped films, the Cu 2p spectra were recoded and are displayed in Fig. S9. The Cu 2p doublet is well resolved. The Cu 2p3/2 peak at 934.6 eV and the satellite at higher binding energies indicate that Cu is oxidized and can be identified as Cu^{+2} ions in octahedral coordination.[54,67,68] The intensity of the Cu 2p3/2 peak for the 3% Cu–2% Li $NiCo_2O_4$ is low, and the satellite structure is not resolved. Nevertheless, the peak is located at BEs around 934.6 eV; thus, even for a lower concentration of Cu, there are Cu^{+2} ions. Table III summarizes

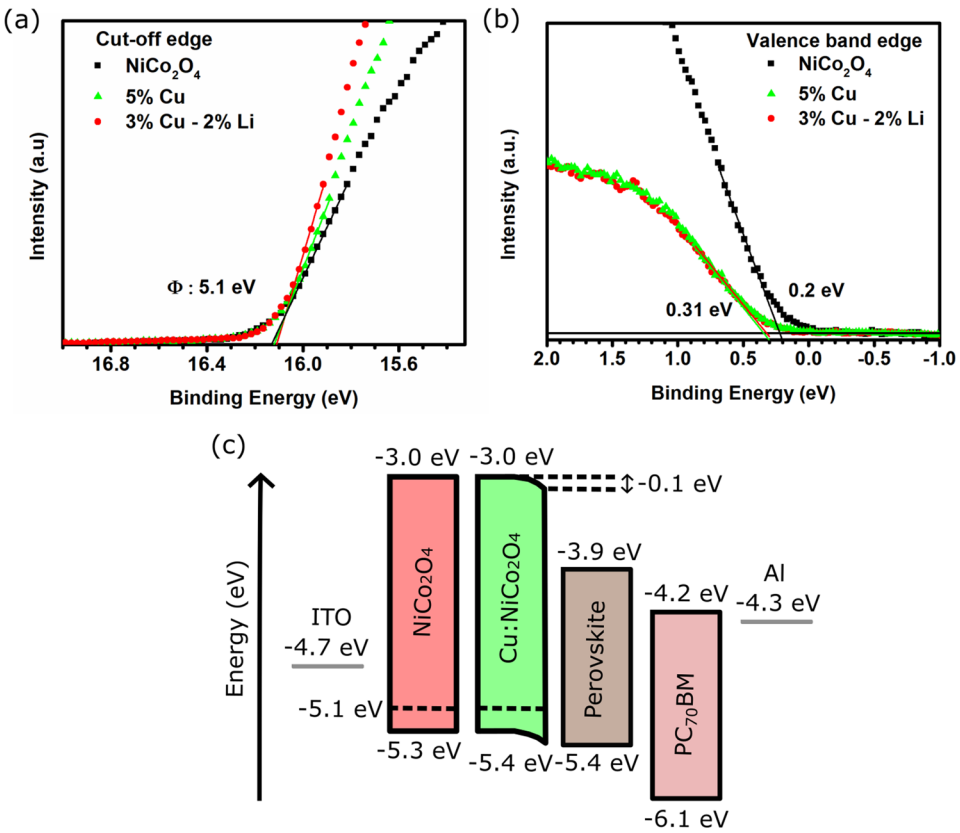

FIG. 3. (a) The high binding energy region and (b) valance band region near the Fermi level of the UPS spectra of undoped, 5% Cu, and 3% Cu–2% Li co-doped $NiCo_2O_4$ HTLs. (c) Schematic representation of energy band levels of the corresponding perovskite solar cells incorporating 5% Cu and 3% Cu–2% Li doped $NiCo_2O_4$ (green bar) and undoped $NiCo_2O_4$ HTLs (red bar). In the case of the doped $NiCo_2O_4$, the band bending indicates the cathodic polarization effect at the surface region of the doped $NiCo_2O_4$ HTL.

the Ni:Co atomic ratio values obtained from the processing of the reported XPS spectra. The surface sensitivity of XPS and material precursor stoichiometry reveal that a small excess of Ni ions is identified at the surface of the undoped $NiCo_2O_4$ as the XPS calculated Ni:Co ratio is 0.55. For 5% Cu doped and 3% Cu–2% Li $NiCo_2O_4$, a decrease in the Ni:Co ratio confirms the deficiency of the Ni ion at the surface, resulting in 0.43 and 0.45 ratios, respectively, which has been preferentially replaced by the Cu ions. These findings agree with the previously reported results of Tavares *et al.*[54] where the introduction of Cu replaces surface Ni ions at the $NiCo_2O_4$ electrodes, which indeed induces a similar effect to cathodic polarization (downshift of the energy bands).

Additional ultraviolet photoelectron spectroscopy (UPS) measurements were also performed on doped and undoped $NiCo_2O_4$ films to determine the energy levels. Figure 3(b) displays the UPS spectra of the valence band region near the Fermi level. The valence band maximum (VBM) for $NiCo_2O_4$ was found at 0.2 eV below the Fermi level, while it is shifted to higher binding energies (~0.3 eV) when $NiCo_2O_4$ is doped with 5% Cu and 3% Cu–2% Li. Figure 1(a) shows the high binding energy region of UPS spectra, where the high energy cut-off region is used to determine the work function (Φ) of the interface. Φ for all films of $NiCo_2O_4$ was found at 5.1 eV, and the ionization potential was calculated by adding the values of Φ and VBM. Thus, ionization potentials were found to be ~5.3 eV for the undoped $NiCo_2O_4$ and ~5.4 eV for 5% Cu and 3% Cu–2% Li $NiCo_2O_4$ HTLs. A schematic representation of PVSC energy band levels applying different types of $NiCo_2O_4$ layers is illustrated in Fig. 3(c) where the calculated values from the UPS and E_g (~2.3 eV) from UV-Vis optical absorption spectra were utilized. To summarize, the induced cathodic polarization of the 3% Cu–2% Li $NiCo_2O_4$ HTL increases the built-in potential of the corresponding PVSCs as shown using Mott-Schottky measurements and reduces the charge recombination losses (as inferred from the EIS results presented) due to better hole extraction (as inferred from the PL measurements presented), giving rise to an increase in both Voc and Jsc compared to undoped $NiCo_2O_4$ HTL based PVSC.

In conclusion, we report the doping of co-doped $NiCo_2O_4$ with 5% Cu and 3% Cu–2% Li to increase the PCE of inverted PVSC using a 350 nm $Pb(CH_3CO_2)_2.3H_2O$:methylammonium iodide (1:3) based perovskite formulation. 5% Cu doping increases the Voc of the corresponding PVSC but decreases the Jsc compared to undoped $NiCo_2O_4$ PVSC due to lower electrical conductivity. To overcome this effect, 3% Cu–2% Li co-doping was applied on solution combustion synthesized $NiCo_2O_4$-HTL, inducing an increase in electrical conductivity, resulting in inverted PVSCs with lower charge transport resistance compared to 5% Cu doped $NiCo_2O_4$-HTL based PVSCs and higher charge recombination resistance compared to undoped $NiCo_2O_4$-HTL based PVSCs. Mott-Schottky measurements showed the higher built-in potential of the Cu doped $NiCo_2O_4$ PVSC, while PL studies confirmed the better hole extraction of the 3% Cu–2% Li $NiCo_2O_4$-HTL/perovskite active layer interface. Further investigation for the origin of this enhancement was performed by XPS measurements on the co-doped and undoped $NiCo_2O_4$, revealing the tendency of Cu ions to replace preferably the surface Ni ions of $NiCo_2O_4$, changing the surface stoichiometry of Ni:Co which induces a cathodic polarization effect. UPS measurements revealed the increase in the ionization potential by 0.1 eV for the 3% Cu–2% Li $NiCo_2O_4$ HTLs compared to undoped $NiCo_2O_4$-HTLs, a parameter which improves hole carrier extraction properties for the 3% Cu–2% Li $NiCo_2O_4$-HTL based PVSCs reported. As a result, inverted PVSCs containing 3% Cu–2% Li co-doped $NiCo_2O_4$ HTL showed an increased PCE of 16.54% compared to undoped $NiCo_2O_4$-HTL based PVSCs with a PCE of 11.61%.

See supplementary material for details of the proposed hole transporting layer materials, processing of perovskite films, and fabrication of perovskite devices. Additional information of material optical characterization, surface topography, XRD and UPS/XPS measurements, and analysis of the experimental results is included.

This project received funding from the European Research Council (ERC) under the European Union's Horizon 2020 research and innovation program (Grant Agreement No. 647311). The authors would like to thank Associate Professor Gregorios Itskos for fruitful discussions.

REFERENCES

[1] A. Kojima, K. Teshima, Y. Shirai, and T. Miyasaka, J. Am. Chem. Soc. **131**, 6050 (2009).
[2] X. Zhu, D. Yang, R. Yang, B. Yang, Z. Yang, X. Ren, J. Zhang, J. Niu, J. Feng, and S. (Frank) Liu, Nanoscale **9**, 12316 (2017).
[3] F. Zhang, Z. Wang, H. Zhu, N. Pellet, J. Luo, C. Yi, X. Liu, H. Liu, S. Wang, X. Li, Y. Xiao, S. M. Zakeeruddin, D. Bi, and M. Grätzel, Nano Energy **41**, 469 (2017).
[4] W. S. Yang, B.-W. Park, E. H. Jung, N. J. Jeon, Y. C. Kim, D. U. Lee, S. S. Shin, J. Seo, E. K. Kim, J. H. Noh, and S. Il Seok, Science **356**, 1376 (2017).
[5] T. Singh and T. Miyasaka, Adv. Energy Mater. **8**, 1700677 (2018).
[6] N. J. Jeon, J. H. Noh, Y. C. Kim, W. S. Yang, S. Ryu, and S. Il Seok, Nat. Mater. **13**, 897 (2014).
[7] D. P. McMeekin, G. Sadoughi, W. Rehman, G. E. Eperon, M. Saliba, M. T. Horantner, A. Haghighirad, N. Sakai, L. Korte, B. Rech, M. B. Johnston, L. M. Herz, and H. J. Snaith, Science **351**, 151 (2016).
[8] F. Hao, C. C. Stoumpos, D. H. Cao, R. P. H. Chang, and M. G. Kanatzidis, Nat. Photonics **8**, 489 (2014).
[9] G. E. Eperon, V. M. Burlakov, P. Docampo, A. Goriely, and H. J. Snaith, Adv. Funct. Mater. **24**, 151 (2014).
[10] M. Saliba, T. Matsui, K. Domanski, J. Y. Seo, A. Ummadisingu, S. M. Zakeeruddin, J. P. Correa-Baena, W. R. Tress, A. Abate, A. Hagfeldt, and M. Grätzel, Science **354**, 206 (2016).
[11] N. J. Jeon, J. H. Noh, W. S. Yang, Y. C. Kim, S. Ryu, J. Seo, and S. Il Seok, Nature **517**, 476 (2015).
[12] M. Liu, M. B. Johnston, and H. J. Snaith, Nature **501**, 395 (2013).
[13] D. Liu and T. L. Kelly, Nat. Photonics **8**, 133 (2014).
[14] J. Burschka, N. Pellet, S. J. Moon, R. Humphry-Baker, P. Gao, M. K. Nazeeruddin, and M. Grätzel, Nature **499**, 316 (2013).
[15] Q. Chen, H. Zhou, Z. Hong, S. Luo, H. S. Duan, H. H. Wang, Y. Liu, G. Li, and Y. Yang, J. Am. Chem. Soc. **136**, 622 (2014).
[16] D. Bi, S.-J. Moon, L. Häggman, G. Boschloo, L. Yang, E. M. J. Johansson, M. K. Nazeeruddin, M. Grätzel, and A. Hagfeldt, RSC Adv. **3**, 18762 (2013).
[17] F. Huang, Y. Dkhissi, W. Huang, M. Xiao, I. Benesperi, S. Rubanov, Y. Zhu, X. Lin, L. Jiang, Y. Zhou, A. Gray-Weale, J. Etheridge, C. R. McNeill, R. A. Caruso, U. Bach, L. Spiccia, and Y. B. Cheng, Nano Energy **10**, 10 (2014).

[18]X. Li, D. Bi, C. Yi, J.-D. Decoppet, J. Luo, S. M. Zakeeruddin, A. Hagfeldt, and M. Gratzel, Science **353**, 58 (2016).
[19]C. W. Chen, H. W. Kang, S. Y. Hsiao, P. F. Yang, K. M. Chiang, and H. W. Lin, Adv. Mater. **26**, 6647 (2014).
[20]A. Ioakeimidis, C. Christodoulou, M. Lux-Steiner, and K. Fostiropoulos, J. Solid State Chem. **244**, 20 (2016).
[21]H. A. Abbas, R. Kottokkaran, B. Ganapathy, M. Samiee, L. Zhang, A. Kitahara, M. Noack, and V. L. Dalal, APL Mater. **3**, 016105 (2015).
[22]P. Docampo, J. M. Ball, M. Darwich, G. E. Eperon, and H. J. Snaith, Nat. Commun. **4**, 2761 (2013).
[23]B. Conings, L. Baeten, C. De Dobbelaere, J. D'Haen, J. Manca, and H. G. Boyen, Adv. Mater. **26**, 2041 (2014).
[24]H. P. Zhou, Q. Chen, G. Li, S. Luo, T. B. Song, H. S. Duan, Z. R. Hong, J. B. You, Y. S. Liu, and Y. Yang, Science **345**, 542 (2014).
[25]J.-H. Im, C.-R. Lee, J.-W. Lee, S.-W. Park, and N.-G. Park, Nanoscale **3**, 4088 (2011).
[26]H.-S. Kim, C.-R. Lee, J.-H. Im, K.-B. Lee, T. Moehl, A. Marchioro, S.-J. Moon, R. Humphry-Baker, J.-H. Yum, J. E. Moser, M. Grätzel, and N.-G. Park, Sci. Rep. **2**, 591 (2012).
[27]L. E. Polander, P. Pahner, M. Schwarze, M. Saalfrank, C. Koerner, and K. Leo, APL Mater. **2**, 081503 (2014).
[28]O. Malinkiewicz, A. Yella, Y. H. Lee, G. M. M. Espallargas, M. Graetzel, M. K. Nazeeruddin, and H. J. Bolink, Nat. Photonics **8**, 128 (2014).
[29]M. Ye, C. He, J. Iocozzia, X. Liu, X. Cui, X. Meng, M. Rager, X. Hong, X. Liu, and Z. Lin, J. Phys. D. Appl. Phys. **50**, 373002 (2017).
[30]V. Zardetto, B. L. Williams, A. Perrotta, F. Di Giacomo, M. A. Verheijen, R. Andriessen, W. M. M. Kessels, and M. Creatore, Sustain. Energy Fuels **1**, 30 (2017).
[31]Z. H. Bakr, Q. Wali, A. Fakharuddin, L. Schmidt-Mende, T. M. Brown, and R. Jose, Nano Energy **34**, 271 (2017).
[32]T. Y. Wen, S. Yang, P. F. Liu, L. J. Tang, H. W. Qiao, X. Chen, X. H. Yang, Y. Hou, and H. G. Yang, Adv. Energy Mater. **8**, 1703143 (2018).
[33]D. Ouyang, J. Xiao, F. Ye, Z. Huang, H. Zhang, L. Zhu, J. Cheng, and W. C. H. Choy, Adv. Energy Mater. **8**, 1702722 (2018).
[34]L. J. Tang, X. Chen, T. Y. Wen, S. Yang, J. J. Zhao, H. W. Qiao, Y. Hou, and H. G. Yang, Chem. - A Eur. J. **24**, 2845 (2018).
[35]F. Galatopoulos, A. Savva, I. T. Papadas, and S. A. Choulis, APL Mater. **5**, 076102 (2017).
[36]K. Yao, F. Li, Q. He, X. Wang, Y. Jiang, H. Huang, and A. K. Y. Jen, Nano Energy **40**, 155 (2017).
[37]W. Chen, Y. Wu, J. Fan, A. B. Djurišić, F. Liu, H. W. Tam, A. Ng, C. Surya, W. K. Chan, D. Wang, and Z. B. He, Adv. Energy Mater. **8**, 1703519 (2018).
[38]W. Sun, Y. Li, S. Ye, H. Rao, W. Yan, H. Peng, Y. Li, Z. Liu, S. Wang, Z. Chen, L. Xiao, Z. Bian, and C. Huang, Nanoscale **8**, 10806 (2016).
[39]H. Rao, S. Ye, W. Sun, W. Yan, Y. Li, H. Peng, Z. Liu, Z. Bian, Y. Li, and C. Huang, Nano Energy **27**, 51 (2016).
[40]A. Savva, I. T. Papadas, D. Tsikritzis, G. S. Armatas, S. Kennou, and S. A. Choulis, J. Mater. Chem. A **5**, 20381 (2017).
[41]J. A. Christians, R. C. M. Fung, and P. V. Kamat, J. Am. Chem. Soc. **136**, 758 (2014).
[42]N. Wijeyasinghe, A. Regoutz, F. Eisner, T. Du, L. Tsetseris, Y.-H. Lin, H. Faber, P. Pattanasattayavong, J. Li, F. Yan, M. A. McLachlan, D. J. Payne, M. Heeney, and T. D. Anthopoulos, Adv. Funct. Mater. **27**, 1701818 (2017).
[43]I. T. Papadas, A. Savva, A. Ioakeimidis, P. Eleftheriou, G. S. Armatas, and S. A. Choulis, Mater. Today Energy **8**, 57 (2018).
[44]H. Zhang, H. Wang, H. Zhu, C. Chueh, W. Chen, S. Yang, and A. K.-Y. Jen, Adv. Energy Mater. **8**, 1702762 (2018).
[45]I. T. Papadas, A. Ioakeimidis, G. S. Armatas, and S. A. Choulis, Adv. Sci. **5**, 1701029 (2018).
[46]I. Zarazua, J. Bisquert, and G. Garcia-Belmonte, J. Phys. Chem. Lett. **7**, 525 (2016).
[47]J.-P. Correa-Baena, W. Tress, K. Domanski, E. H. Anaraki, S.-H. Turren-Cruz, B. Roose, P. P. Boix, M. Grätzel, M. Saliba, A. Abate, and A. Hagfeldt, Energy Environ. Sci. **10**, 1207 (2017).
[48]D. Liu, S. Li, P. Zhang, Y. Wang, R. Zhang, H. Sarvari, F. Wang, J. Wu, Z. Wang, and Z. D. Chen, Nano Energy **31**, 462 (2017).
[49]B.-X. Chen, H.-S. Rao, W.-G. Li, Y.-F. Xu, H.-Y. Chen, D.-B. Kuang, and C.-Y. Su, J. Mater. Chem. A **4**, 5647 (2016).
[50]S. S. Shin, E. J. Yeom, W. S. Yang, S. Hur, M. G. Kim, J. Im, J. Seo, J. H. Noh, and S. Il Seok, Science **356**, 167 (2017).
[51]J. H. Kim, P.-W. Liang, S. T. Williams, N. Cho, C.-C. Chueh, M. S. Glaz, D. S. Ginger, and A. K.-Y. Jen, Adv. Mater. **27**, 695 (2015).
[52]W. Chen, Y. Wu, Y. Yue, J. Liu, W. Zhang, X. Yang, H. Chen, E. Bi, I. Ashraful, M. Gratzel, and L. Han, Science **350**, 944 (2015).
[53]M.-H. Liu, Z.-J. Zhou, P.-P. Zhang, Q.-W. Tian, W.-H. Zhou, D.-X. Kou, and S.-X. Wu, Opt. Express **24**, A1349 (2016).
[54]A. Tavares, M. da Silva Pereira, M. Mendonça, M. Nunes, F. Costa, and C. Sá, J. Electroanal. Chem. **449**, 91 (1998).
[55]A. Guerrero, G. Garcia-Belmonte, I. Mora-Sero, J. Bisquert, Y. S. Kang, T. J. Jacobsson, J.-P. Correa-Baena, and A. Hagfeldt, J. Phys. Chem. C **120**, 8023 (2016).
[56]H.-S. Kim, I.-H. Jang, N. Ahn, M. Choi, A. Guerrero, J. Bisquert, and N.-G. Park, J. Phys. Chem. Lett. **6**, 4633 (2015).
[57]J.-H. Kim, H. Y. Lee, and J.-Y. Lee, J. Nanosci. Nanotechnol. **18**, 2021 (2018).
[58]P. P. Boix, G. Garcia-Belmonte, U. Muñecas, M. Neophytou, C. Waldauf, and R. Pacios, Appl. Phys. Lett. **95**, 233302 (2009).
[59]A. Guerrero, J. You, C. Aranda, Y. S. Kang, G. Garcia-Belmonte, H. Zhou, J. Bisquert, and Y. Yang, ACS Nano **10**, 218 (2016).
[60]D. Zhao, M. Sexton, H.-Y. Park, G. Baure, J. C. Nino, and F. So, Adv. Energy Mater. **5**, 1401855 (2015).
[61]W. Shockley and W. T. Read, Phys. Rev. **87**, 835 (1952).
[62]R. N. Hall, Phys. Rev. **87**, 387 (1952).
[63]M. M. Mandoc, F. B. Kooistra, J. C. Hummelen, B. de Boer, and P. W. M. Blom, Appl. Phys. Lett. **91**, 263505 (2007).
[64]S. R. Cowan, A. Roy, and A. J. Heeger, Phys. Rev. B **82**, 245207 (2010).
[65]J. F. Marco, J. R. Gancedo, M. Gracia, J. L. Gautier, E. Ríos, and F. J. Berry, J. Solid State Chem. **153**, 74 (2000).
[66]T. J. Chuang, C. R. Brundle, and D. W. Rice, Surf. Sci. **59**, 413 (1976).
[67]A. C. Tavares, M. A. M. Cartaxo, M. I. da Silva Pereira, and F. M. Costa, J. Solid State Electrochem. **5**, 57 (2001).
[68]A. C. Tavares, M. A. M. Cartaxo, M. I. Da Silva Pereira, and F. M. Costa, J. Electroanal. Chem. **464**, 187 (1999).